

ChemComm

Accepted Manuscript



This is an *Accepted Manuscript*, which has been through the Royal Society of Chemistry peer review process and has been accepted for publication.

Accepted Manuscripts are published online shortly after acceptance, before technical editing, formatting and proof reading. Using this free service, authors can make their results available to the community, in citable form, before we publish the edited article. We will replace this *Accepted Manuscript* with the edited and formatted *Advance Article* as soon as it is available.

You can find more information about *Accepted Manuscripts* in the [Information for Authors](#).

Please note that technical editing may introduce minor changes to the text and/or graphics, which may alter content. The journal's standard [Terms & Conditions](#) and the [Ethical guidelines](#) still apply. In no event shall the Royal Society of Chemistry be held responsible for any errors or omissions in this *Accepted Manuscript* or any consequences arising from the use of any information it contains.

COMMUNICATION

Ultrafast liquid water transport through graphene-based nanochannels measured by isotope labelling

Cite this: DOI: 10.1039/x0xx00000x

Pengzhan Sun,^a He Liu,^b Kunlin Wang,^a Minlin Zhong,^a Dehai Wu^b and Hongwei Zhu^{a,c}

Received 00th January 2014,

Accepted 00th January 2015

DOI: 10.1039/x0xx00000x

www.rsc.org/

Based on isotope labelling, we found that liquid water can afford an ultrafast permeation through graphene-based nanochannels with a diffusion coefficient 4–5 orders of magnitude greater than the bulk case. When dissolving ions in sources, the diffusion coefficient of ions through graphene channels lies in the same order of magnitude as water, while the ion diffusion is slightly faster than water, indicating that the ions are mainly transported by water flows and the delicate interactions between ions and nanocapillary walls also take effect in the accelerated ion transportation.

Mass transport through materials with nanoscaled pores or channels is currently an attractive subject with significant implications in nanofluidic device design and the fundamental understanding of fluids at nanoscale.^{1,2} Carbon nanomaterials, *e.g.* carbon nanotubes^{3–7} and graphene oxide (GO) membranes^{8,9}, with numerous hydrophobic graphitic nanochannels inside, can afford an ultrafast transport of water molecules. Recently, GO membranes are reported with the ability to separate different ions in solutions with an ultrafast speed based on the physical size effect of nanocapillaries^{10,11} and the diverse interactions between ions and GO membranes^{12–15}. In combination with the characteristics of easy to synthesize and scale up,^{16,17} GO membranes are believed to have great promises in the fabrication of filtration membranes for waste water treatment and the simplified nanofluidic platforms for biomimetic selective mass transportation. Typically, in contrast to GO layers with a nanometer-sized thickness,^{18–21} in which mass transport happens mostly through the structural defects within GO flakes, as-synthesized micrometer-thick GO membranes are impermeable to most of the liquids and gases (including helium). Exceptionally, water vapors can afford an unimpeded permeation through the *sp*² nanocapillary networks formed by connecting all the stacking layers across the whole laminates,^{8,9} and small ions (hydrated radii < 0.45 nm) can also permeate through with an ultrafast speed.¹⁰ In spite of these exciting results obtained with GO membranes, the permeation behavior of liquid

water, which is a much more complex system than the gaseous state, is unclear; that is the most fundamental problem and of crucial importance for mass transport in solutions.

The investigation of liquid water permeation under no external hydrostatic pressure remains to be a challenge, because no detectable differences in both macroscopic and microscopic levels are present between sources and drains separated by the central GO membranes. To overcome this issue, a novel isotope labelling technique is utilized in this study, in which certain amount of deuterium oxide (D₂O) is dissolved as a tracer to label the source water and the trans-membrane permeation of D₂O is investigated to extrapolate that of water. Based on this isotope labelling technique, not only the permeation behavior of liquid water through the nanocapillaries within GO membranes can be monitored, but also the transport properties of solvent water in the presence of dissolved ions can be studied. These fundamental problems for GO membrane-based mass transportation in aqueous solutions haven't been reported thus far, which are specially investigated with the assistance of isotope labelling technique in this work.

GO sheets were synthesized by the modified Hummers' method starting from natural graphitic flakes, which were exposed to potassium permanganate, sodium nitrite and concentrated sulfuric acid subsequently.²² Figure S1 shows the SEM and AFM characterizations of as-synthesized GO flakes, revealing that the GO flakes are single-layered with a typical lateral dimension of ~1 μm. After dissolving the GO flakes in water by sonication, micrometer-thick GO membranes were prepared by vacuum filtration with commonly used cellulose microfilters (pore size: ~220 nm, porosity: ~80%), as illustrated in Fig. 1a. Typically, a network of ultralong and tortuous *sp*² nanocapillaries is formed within the micrometer-thick GO laminates, which is responsible for the transport of water molecules and ions.^{8–11,23} The leakage through the structural defects within GO flakes is believed to be negligible due to the mutual stacking of several thousand GO layers.²³ This has been further confirmed by varying the lateral dimensions of GO flakes within the membranes from micrometer to nanometer, which yields an enhancement of ion transportation.^{13,15} In contrast, for

the case of nanometer-thick GO membranes, in which only few layers of GO flakes are stacked together, the expected continuous nanocapillary networks are hardly to form and the mass transport is dominated by the structural defects within the GO flakes.^{18,19} Hence, for the micrometer-thick GO membranes used in all the experiments here, the sp^2 nanocapillaries formed within the laminates are mainly responsible for the water and ion transportations, as sketched in Fig. 1a.

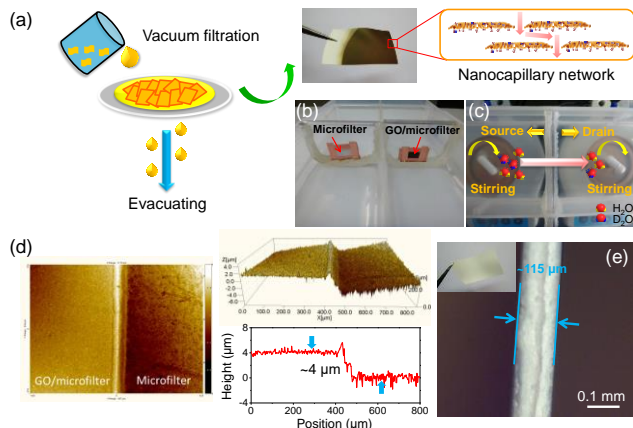


Figure 1. (a) Left panel: schematic drawing for the fabrication of GO membranes by vacuum-filtration. Right panel: a photograph for the as-synthesized GO membrane and a schematic diagram for its cross-sectional structure. (b, c) Photographs for the home-made permeation apparatus and the D_2O labelled water trans-membrane permeation process. (d) White light interference characterizations for the interface between GOCM and microfilter membrane. (e) An optical image for the cross-section of cellulose microfilter. The inset shows a photograph of the microfilter used in the experiments.

Following the membrane preparation procedure, the GO membrane with the cellulose microfilter underneath (named as “GOCM”) was assembled into a home-made permeation apparatus, as shown in Fig. 1b.²⁴ Note that the GO membranes were not detached off from the microfilters, considering the fact that the underneath polymeric substrates could provide a significant mechanical strength enhancement to ensure that the GO membranes were not damaged during water permeation. The intactness and continuity of the GO membranes were also checked by optical microscopy before and after experiments. To extract the effect of the substrates on water permeation, control experiments were conducted with blank microfilters, as shown in Fig. 1b. In the water permeation experiments, 100 mL of D_2O labelled water with various mass concentrations and deionized water were injected into the source and drain reservoirs, respectively. The whole water permeation process was conducted under mild magnetic stirring, as shown in Fig. 1c, to avoid possible D_2O concentration gradients around the membranes. The filtrates in drains were examined by Fourier transform infrared (FTIR) spectroscopy to afford accurate concentrations of D_2O tracers (discuss later), based on which the permeation behavior of liquid water could be extrapolated. Figure 1d exhibits the interface topography between GOCM and microfilter obtained by the white light interference microscope, from which the thickness of the GO membranes (prepared by vacuum-filtrating 25 mL, 0.1 mg/mL GO solutions) was determined as $\sim 4 \mu\text{m}$, which has also been confirmed by stylus profilometry, as shown in Fig. S2. The thickness of the cellulose microfilters used here was evaluated by the cross-section optical microscopy, as shown in Fig. 1e, which reveals that the microfilters possess a thickness of $\sim 115 \mu\text{m}$.

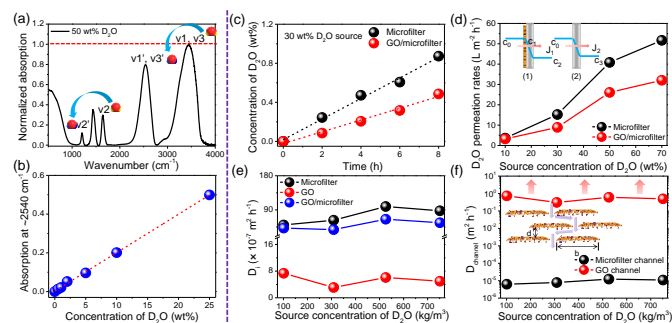


Figure 2. (a) FTIR spectrum of a 50 wt% D_2O solution. (b) Functional relationship between the absorption intensity at $\sim 2540 \text{ cm}^{-1}$ and the mass concentration of D_2O in solutions. (c) D_2O mass transportations *versus* time through GOCM and blank microfilter membranes with a source D_2O concentration of 30 wt%. (d) D_2O permeation rates through GOCM and blank microfilter membranes as a function of the source concentration. The inset shows the schematic diagrams for the calculation of diffusion coefficients through GO and microfilters by Fick's first law. (e) D_2O diffusion coefficients through the entire GO, microfilter and GOCM membranes as a function of the D_2O source concentration. (f) D_2O diffusion coefficients through the channels within GO and microfilters as a function of the D_2O source concentration. The inset shows a schematic diagram for the cross-section of GO membranes used for calculation. The red arrows indicate the lower bounds for the water diffusion coefficients.

To measure the concentration of D_2O tracers in drain solutions, FTIR spectroscopy was utilized. Figure 2a shows an example of the FTIR spectrum of 50 wt% D_2O solution. Typically, gaseous water is a nonlinear three-atomic molecule and its FTIR spectrum exhibits three characteristic peaks located at $\nu_1 = \sim 3652 \text{ cm}^{-1}$, $\nu_2 = \sim 1596 \text{ cm}^{-1}$ and $\nu_3 = \sim 3756 \text{ cm}^{-1}$, respectively. However, due to the strong hydrogen bonding effect in liquid water, the extension vibration modes of ν_1 and ν_3 overlap together to form a wide peak located at $\sim 3440 \text{ cm}^{-1}$, while the angular vibration mode ν_2 is located at $\sim 1645 \text{ cm}^{-1}$. On the other hand, in the case of D_2O , due to the slightly larger atomic mass of deuterium than hydrogen, the overlapped peak corresponding to extension vibration modes (ν_1' and ν_3') shifts to $\sim 2540 \text{ cm}^{-1}$ and the angular vibration mode ν_2' shifts to $\sim 1210 \text{ cm}^{-1}$ (Fig. 2a). Therefore, based on the absorption intensity of the characteristic peak located at $\sim 2540 \text{ cm}^{-1}$ in the FTIR spectra, the accurate concentration of D_2O tracers in drains can be determined. Firstly, the FTIR spectra of D_2O aqueous solutions with fixed mass concentrations were carried out to quantify the function between the absorption intensity at $\sim 2540 \text{ cm}^{-1}$ and the mass concentration of D_2O in solutions (Fig. S3). The obtained FTIR spectra were baselined and normalized with the overlapped peak located at $\sim 3440 \text{ cm}^{-1}$ (Figs. 2a and S3) and the absorption intensities located at $\sim 2540 \text{ cm}^{-1}$ were plotted as a function of the mass concentrations, as shown in Fig. 2b. It reveals that the absorption intensity at $\sim 2540 \text{ cm}^{-1}$ (A) varies linearly with the mass concentration of D_2O (c_m), following a function of $A = 0.01983 c_m$. With this linear function, the D_2O labelled water permeation properties through GO membranes can be investigated, as shown in Figs. 2c-f. An example of the relationship of D_2O mass transport *versus* time is plotted in Fig. 2c (the source concentration of D_2O in this case is 30 wt% and D_2O permeations with other source concentrations of 10~70 wt% are shown and compared in Fig. S4). For each group of experiments, where water sources with different D_2O concentrations were allowed to permeate through GOCM and blank microfilter respectively, at least three runs were repeated. Excellent reproducibility could be obtained and the data can be well fitted into a linear relationship. As shown in Figs. 2c and S4,

substantial deviations occur between the D₂O permeations through GOCM and microfilter. With the gradual decrease of the D₂O source concentration, the differences in D₂O permeations through GOCM and the control membrane become smaller. Surprisingly, when the source concentration of D₂O is down to 10 wt%, the permeations of trace quantity D₂O through these two membranes nearly coincide together, just like in the absence of GO membrane; that is, for the blank microfilter. This indicates that liquid water can afford an ultrafast permeation through GO membranes, in spite of the complex interactions among water molecules in the liquid phase, just the same as water vapor,⁸ and also in consistent with the mass transport properties observed in carbon nanotubes.³⁻⁷ Additional experiments with even lower D₂O concentrations were also performed and it's found that the amount of D₂O in drains was failed to detect accurately, indicating that 10 wt% is a lower bound for the observation of D₂O labelled water flow through GO membranes.

As shown in Figs. 2c and S4, after 8 h of permeation, the amount of D₂O in drains only increases to < 5% compared to source concentrations. This means that water trans-membrane permeation can be treated as a quasi-static process, in which the Fick's first law can be utilized to calculate the diffusion coefficients of D₂O through GO membranes and microfilters, as illustrated in the inset of Fig. 2d.²⁴ Firstly, the flow rates of D₂O through GOCM and blank microfilter membranes were calculated, as shown in Fig. 2d. It reveals that reducing the source concentration yields the decrease of the D₂O permeation rates as well as the deviations between the permeations through GOCM and microfilter membranes. With the D₂O flow rates through GOCM and microfilter membranes (Fig. 2d), the diffusion coefficients of D₂O through microfilter, GO and GOCM membranes are calculated, and utilized to extrapolate the cases of liquid water, as plotted in Fig. 2e.²⁴ It reveals that the diffusion coefficients of D₂O through GO membranes are smaller than through microfilters by ~1 order of magnitude when the source concentration is varied from 10 wt% to 70 wt%. At first glance, one may conclude that such a small diffusion coefficient of water through GO membranes makes it even less promising than the commonly used cellulose microfilters. However, if the microstructure of GO membranes is considered, we can draw a rather different conclusion. In view of the structure of GO sheet, nanosized *sp*² clusters are distributed randomly within the *sp*³ C-O matrix.^{25,26} When a large amount of GO flakes are stacked together to form the micrometer-thick laminate, numerous millimeter-long graphitic nanocapillaries can be formed by connecting the *sp*² clusters across all the stacking layers,²⁴ which are responsible for the transport of water, as illustrated in the inset of Fig. 2f. The role of *sp*²-nanocapillaries for water-based mass transport was first proposed and demonstrated by the work of Geim group^{8,10}, which has also been confirmed in our previous work of selective ion trans-membrane transportation in aqueous solutions by varying the lateral dimensions of as-stacked GO flakes from micrometer size to several hundred nanometer size. We found that the ion permeation rates were enhanced proportionally with the reduction of GO flake sizes, further demonstrating the dominant role of the nanocapillary networks formed within micrometer-thick GO laminates for mass transport in solutions (illustrated in the inset of Fig. 2f). On the other hand, this conclusion was further in contrast to the gas transportation cases in the work by Kim, et al.¹⁸ and Li, et al.¹⁹, respectively, in which the gas transportations through nanometer-thick GO membranes were attributed to the structural defects within GO flakes. However, for both cases^{18,19}, only discrete layers of GO flakes were stacked

to form the membranes and the continuous *sp*²-nanocapillary networks cannot be formed, further leading to the selective gas leakage through the structural defects within the GO flakes. Therefore, based on the above reasons, we believe that liquid water diffuses mostly through the nanocapillaries formed within the GO laminates and the leakage through the structural defects is neglected because of mutual stacking, just in consistent with the results published previously.^{8,9,10,17,18,23} Similarly, in the case of microfilters with porosities of ~80%, water diffusions happen mostly through the sub-micrometer-sized pores (~0.22 μm) within the matrix. Based on the microstructures of GO and cellulose microfilters, the diffusion coefficients of D₂O through the channels within GO and microfilters are calculated according to the previous method used in the work by Nair, et al.⁸ and Joshi, et al.¹⁰, which has been proved to provide sufficient matches with the experimental results and molecular dynamics calculations, as plotted in Fig. 2f.²⁴ Surprisingly, the water diffusion coefficients through the nanochannels within GO membranes are 4~5 orders of magnitude greater than through the sub-micrometer-sized cellulose pores, just similar to the cases of water transport through the inner graphitic channels within carbon nanotubes.³⁻⁶ Note that the calculated water diffusion coefficients through the nanochannels within GO membranes are lower bounds because i) recent simulation results have predicted that the functionalized C-O regions within the GO sheets suppress water permeation;^{27,28} ii) the cellulose microfilters possess a rough surface morphology and the bottom GO sheets are likely to insert into the pores, further leading to the disordered arrangement of the GO sheets underneath and the thickening of the whole GO layers (beyond the well-stacking thickness of 4 μm).^{29,30}

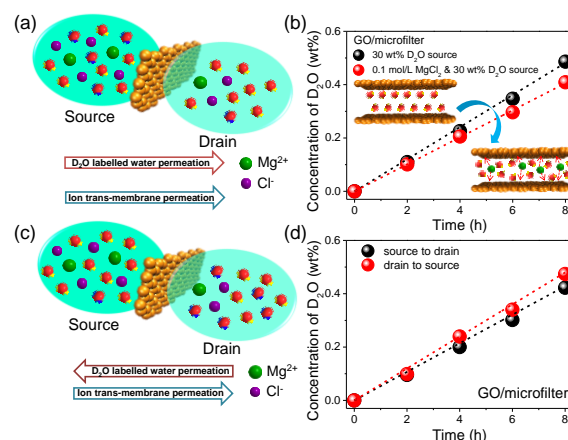


Figure 3. (a, c) Schematic drawings for the labelling of 0.1 M MgCl₂ source solution and the corresponding drain solution by 30 wt% D₂O tracers. (b) Water permeations through GOCM with and without ions in sources. The inset shows the possible mechanism for water permeation in the presence of ions. (d) Water permeations through GOCM in both directions when dissolving ions in sources.

Specially, the water permeation properties through GO membranes when dissolving ions in solutions were investigated based on 0.1 M MgCl₂ sources and 30 wt% D₂O tracers, as shown in Fig. 3. Firstly, the 0.1 M MgCl₂ source solution was labelled with D₂O tracers to study the forward water transport in the presence of ions, as illustrated in Fig. 3a. It reveals that the water permeation is slightly reduced when ions are dissolved in source solution (Fig. 3b). Previous first-principle calculations have demonstrated that the formation of ice bilayer within the interlayer spacing and its melt transition at the edges of the flakes are responsible for the rapid water transport through GO membranes.⁹ Herein, these theoretical results might also be

applied to explain the water permeations in the presence of ions in nanocapillaries: the existent ions might cause some distortion to the ordered ice bilayer, further yielding the slightly reduced water permeation rates, as sketched in the inset of Fig. 3b. However, in order to confirm this hypothesis, further experimental measurements and theoretical calculations are needed. Next, the drain solution was labelled with 30 wt% D₂O to study the water permeation from drain to source in the presence of source ions, as illustrated in Fig. 3c. Notably, it reveals that the water permeation from drain to source is slightly faster than from source to drain when 0.1 M MgCl₂ is present in source solutions (Fig. 3d). This is attributed to the semipermeable effect of GO membranes,¹⁰ through which water are tended to be transported against the ion concentration gradients. On the other hand, the ion trans-membrane permeations in the presence of D₂O tracers are shown in Figs. S5a-d, indicating that the D₂O molecules in sources or drains have neglected effect on ion permeations. The calculated ion diffusion coefficients for the entire membranes and the channels within the membranes are found to be in the same order of magnitude as water, as shown in Figs. S5e-h. These results suggest that the ions in sources are mainly transported by the fast water flows through GO membranes. Notably, the diffusion coefficients of ions through graphene-based nanochannels are slightly greater than water, indicating that the delicate interactions between ions and GO membranes¹²⁻¹⁵ also take effect in the accelerated ion transportation.

Conclusions

In summary, liquid water transport through graphene-based nanochannels without external hydrostatic pressures has been investigated. Based on isotope labelling, we have shown that liquid water can undergo an ultrafast permeation through the millimeter-long nanocapillaries in GO membranes, in spite of the complex interactions among water molecules in the liquid phase, just similar to the case of carbon nanotubes and water vapors in GO laminates. However, the study on liquid water permeation makes more sense than the gaseous case because it can throw light upon the mechanism of ultrafast selective ion transportation through GO membranes, which is of crucial importance for solution-based mass transport in areas of filtration, separation and biomimetic cellular processes. Also the solution-processed GO membranes are readily to fabricate and scale up. The results present here may indeed lay the foundation on nanofluidic device design and biomimetic fast mass transportation based on engineering the nanochannels within GO membranes.

This work was supported by Beijing Science and Technology Program (D141100000514001) and the Training Program of Innovation and Entrepreneurship for Undergraduates (201410003B046).

Notes and references

^a School of Materials Science and Engineering, State Key Laboratory of New Ceramics and Fine Processing, Tsinghua University, Beijing 100084, China. Email: hongweizhu@tsinghua.edu.cn.

^b Department of Mechanical Engineering, Tsinghua University, Beijing 100084, China.

^c Center for Nano and Micro Mechanics, Tsinghua University, Beijing 100084, China.

Electronic Supplementary Information (ESI) available: details of materials and methods, and supplementary figures. See DOI: 10.1039/c000000x/

- X. Hou, W. Guo, L. Jiang, *Chem. Soc. Rev.* 2011, 40, 2385–2401.
- L. Bocquet, E. Charlaix, *Chem. Soc. Rev.* 2010, 39, 1073–1095.
- J. K. Holt, H. G. Park, Y. Wang, M. Stadermann, A. B. Artyukhin, C. P. Grigoropoulos, A. Noy, O. Bakajin, *Science* 2006, 312, 1034–1037.
- M. Majumder, N. Chopra, R. Andrews, B. J. Hinds, *Nature* 2005, 438, 44.
- M. Whitby, N. Quirke, *Nat. Nanotechnol.* 2007, 2, 87–94.
- J. A. Thomas, A. J. H. McGaughey, *Phys. Rev. Lett.* 2009, 102, 184502.
- X. Qin, Q. Yuan, Y. Zhao, S. Xie, Z. Liu, *Nano Lett.* 2011, 11, 2173–2177.
- R. R. Nair, H. A. Wu, P. N. Jayaram, I. V. Grigorieva, A. K. Geim, *Science* 2012, 335, 442–444.
- D. W. Boukhalov, M. I. Katsnelson, Y.-W. Son, *Nano Lett.* 2013, 13, 3930–3935.
- R. K. Joshi, P. Carbone, F. C. Wang, V. G. Kravets, Y. Su, I. V. Grigorieva, H. A. Wu, A. K. Geim, R. R. Nair, *Science* 2014, 343, 752–754.
- B. Mi, *Science* 2014, 343, 740–742.
- P. Sun, M. Zhu, K. Wang, M. Zhong, J. Wei, D. Wu, Z. Xu, H. Zhu, *ACS Nano* 2013, 7, 428–437.
- P. Sun, F. Zheng, M. Zhu, Z. Song, K. Wang, M. Zhong, D. Wu, R. B. Little, Z. Xu, H. Zhu, *ACS Nano* 2014, 8, 850–859.
- P. Sun, H. Liu, K. Wang, M. Zhong, D. Wu, H. Zhu, *J. Phys. Chem. C* 2014, 118, 19396–19401.
- P. Sun, K. Wang, J. Wei, M. Zhong, D. Wu, H. Zhu, *J. Mater. Chem. A* 2014, 2, 7734–7737.
- D. A. Dikin, S. Stankovich, E. J. Zimney, R. D. Piner, G. H. Dommett, G. Evmenenko, S. T. Nguyen, R. S. Ruoff, *Nature* 2007, 448, 457–460.
- G. Eda, G. Fanchini, M. Chhowalla, *Nat. Nanotechnol.* 2008, 3, 270–274.
- H. W. Kim, H. W. Yoon, S. M. Yoon, B. M. Yoo, B. K. Ahn, Y. H. Cho, H. J. Shin, H. Yang, U. Paik, S. Kwon, J. Y. Choi, H. B. Park, *Science* 2013, 342, 91–95.
- H. Li, Z. Song, X. Zhang, Y. Huang, S. Li, Y. Mao, H. J. Ploehn, Y. Bao, M. Yu, *Science* 2013, 342, 95–98.
- M. Hu, B. Mi, *Environ. Sci. Technol.* 2013, 47, 3715–3723.
- Y. Han, Z. Xu, C. Gao, *Adv. Funct. Mater.* 2013, 23, 3693–3700.
- W. S. Hummers, R. E. Offeman, *J. Am. Chem. Soc.* 1958, 80, 1339.
- K. Huang, G. Liu, Y. Lou, Z. Dong, J. Shen, W. Jin, *Angew. Chem. Int. Ed.* 2014, 53, 1–5.
- See Electronic Supplementary Information Online.
- G. Eda, M. Chhowalla, *Adv. Mater.* 2010, 22, 2392–2415.
- K. P. Loh, Q. Bao, G. Eda, M. Chhowalla, *Nature Chem.* 2010, 2, 1015–1024.
- N. Wei, X. Peng, Z. Xu, *Phys. Rev. E* 2014, 89, 012113.
- N. Wei, X. Peng, Z. Xu, *ACS Appl. Mater. Interfaces* 2014, 6, 5877–5883.
- T.-M. Yeh, Z. Wang, D. Mahajan, B. S. Hsiao, B. Chu, *J. Mater. Chem. A* 2013, 1, 12998–13003.
- Y. Huang, H. Li, L. Wang, Y. Qiao, C. Tang, C. Jung, Y. Yoon, S. Li, M. Yu, *Adv. Mater. Interfaces* 2014, 1400433.